# Biphenylene Dimer. Molecular Fragment of a Two-Dimensional Carbon Net and Double-Stranded Polymer

**Andrzej Rajca,* Andrej Safronov, Suchada Rajca, Charles R. Ross, II, and John J. Stezowski**

*Contribution from the Department of Chemistry, University of Nebraska, Lincoln, Nebraska 68588-0304*

*Received April 1, 1996*[⊗]

**Abstract:** Biphenylene dimers, which may be considered as "macrocyclic" 2 × 2 fragments of net **1** and dimeric fragments of a double-stranded polymer, **5**, are prepared. X-ray crystallography on two polymorphs of the dimer **9** reveals that its bond alternation is analogous to that in biphenylene; the tetraphenylene part of **9** has approximately $C_{2h}$ symmetry with a small dihedral angle (<12°) between the benzene rings in the adjacent biphenylenes. Cyclic voltammetry of **9** gives two reversible waves corresponding to a radical anion and a dianion; the lithium and potassium salts of these anions, $\mathbf{9}^{\bullet-}$,$\mathbf{M}^+$ (M = Li, K) and $\mathbf{9}^{2-}$,$\mathbf{2M}^+$ (M = Li, K), were generated and characterized by ESR, NMR, and UV−vis spectroscopies. The spectral data for the dianions are compatible with classical structures; no evidence for "in-plane aromaticity" is found. For polymer **5**, a localized band and large density of states near the Fermi level are found, using extended Hückel theory calculations.

## Introduction

Graphite, diamond, and fullerenes are well-documented carbon allotropes of great interest in science and technology.[1] Unique bonding features of carbon lead to the design of imaginative and aesthetically pleasing structures for other possible all-carbon networks.[1,2] Most importantly, the search for new carbon allotropes is driven by the promise of novel materials with interesting properties.[1−4] In addition to the well-known hexagonal net of graphite, other two-dimensional (2D) "planar" all-carbon nets of benzene rings (e.g., **1** and **2**) have been proposed.[5]

Nets **1** and **2** may be thought of as structurally related to the following one-dimensional (1D) polymers: "linear" polyphenylene **3**, "angular" polyphenylene **4**, and "double-stranded" poly(*peri*-biphenylene) **5**. Different $\pi$-conjugative properties of the oligomers derived from polymers **3** and **4** have been predicted, with those related to **3** being strongly delocalized and those related to **4** possessing "localized" $\pi$-bonding.[6] "Localization" in **4** may arise as double bonds tend to be exocyclic with respect to the four-membered rings, in order to minimize the antiaromatic character of four-electron $\pi$-bonding within the cyclobutadiene ring.[6,7]

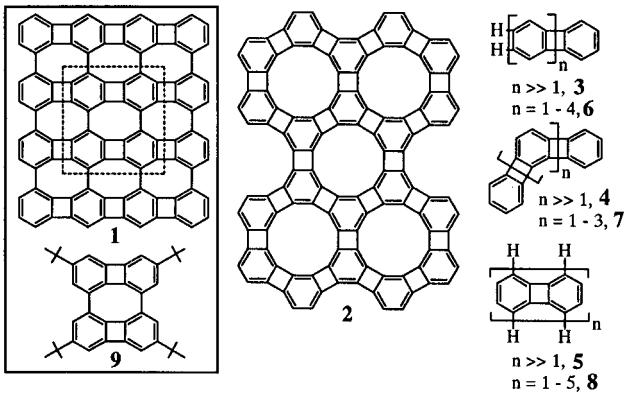


Vollhardt's group has developed efficient synthetic routes for a family of angular and linear oligophenylenes, **6** and **7**.[8−10] Also, oligophenylenes and related structures have been pursued as tests of aromaticity and strain.[8−12]

[⊗] Abstract published in *Advance ACS Abstracts,* July 15, 1996.

(1) Reviews on synthetic approaches to carbon allotropes: (a) Diederich, F.; Rubin, Y. *Angew. Chem., Int. Ed. Engl.* **1992**, *31*, 1101. (b) Diederich, F. *Nature* **1994**, *369*, 199.

(2) For recent leading references on theoretical and experimental work aimed at carbon allotropes, see: Bucknum, M. J.; Hoffmann, R. *J. Am. Chem. Soc.* **1994**, *116*, 11456. Nesper, R.; Vogel, K.; Blochl, P. E. *Angew. Chem., Int. Ed. Engl.* **1993**, *32*, 701. Feldman, K. S.; Weinreb, C. K.; Youngs, W. J.; Bradshaw, J. D. *J. Am. Chem. Soc.* **1994**, *116*, 9019. Kijima, M.; Sakai, Y.; Shirikawa, H. *Chem. Lett.* **1994**, 2011. Anthony, J.; Boudon, C.; Diederich, F.; Gisselbrecht, J.-P.; Gramlich, V.; Gross, M.; Hobi, M.; Seiler, P. *Angew. Chem., Int. Ed. Engl.* **1994**, *33*, 763.

(3) Kroto, H. W.; Heath, J. R.; O'Brien, S. C.; Curl, R. F.; Smalley, R. E. *Nature* **1985**, *318*, 162. Krätschner, W.; Lamb, L. D.; Fostiropoulos, K.; Huffman, D. R. *Nature* **1990**, *347*, 354.

(4) Haddon, R. C.; et al. *Nature* **1991**, *350*, 320. Hebard, A. F.; et al. *Nature* **1991**, *350*, 600. Allemand, P.-M.; Khemani, K. C.; Koch, A.; Wudl, F.; Holczer, K.; Donovan, S.; Gruner, G.; Thompson, J. D. *Science* **1991**, *253*, 301.

(5) Balaban, A. T.; Rentia, C. C.; Ciupitu, E. *Rev. Roum. Chim.* **1968**, *13*, 231. Merz, K. M., Jr.; Hoffmann, R.; Balaban, A. T. *J. Am. Chem. Soc.* **1987**, *109*, 6742. Balaban, A. T. *Comput. Math. Appl.* **1989**, *17*, 397.

(6) Barron, T. H. K.; Barton, J. W.; Johnson, J. D. *Tetrahedron* **1966**, *22*, 2609.

(7) Faust, R.; Glendening, E. D.; Streitwieser, A.; Vollhardt, K. P. C. *J. Am. Chem. Soc.* **1992**, *114*, 8263. Baldridge, K. K.; Siegel, J. S. *J. Am. Chem. Soc.* **1992**, *114*, 9583. Bürgi, H.-B.; Baldridge, K. K.; Hardcastle, K.; Frank, N. L.; Gantzel, P.; Siegel, J. S.; Ziller, J. *Angew. Chem., Int. Ed. Engl.* **1995**, *34*, 1454.

(8) Reviews on phenylenes and related compounds: Vollhardt, K. P. C. *Pure Appl. Chem.* **1993**, *65*, 153. Toda, F.; Garratt, P. *Chem. Rev.* **1992**, *92*, 1686. Cava, M. P.; Mitchell, M. J. *Cyclobutadiene and Related Compounds*; Academic: New York, 1967.

(9) Lothrop, W. C. *J. Am. Chem. Soc.* **1941**, *63*, 1187.

(10) Leading references for linear and angular oligophenylenes: (a) Barton, J. W.; Walker, R. B. *Tetrahedron Lett.* **1978**, 1005. (b) Barton, J. W.; Rowe, D. J. *Tetrahedron Lett.* **1983**, 299. (c) Berris, B. C.; Hovakeemian, G. H.; Lai, Y.-H.; Mestdagh, H.; Vollhardt, K. P. C. *J. Am. Chem. Soc.* **1985**, *107*, 5670. (d) Diercks, R.; Vollhardt, K. P. C. *J. Am. Chem. Soc.* **1986**, *108*, 3150. (e) Blanco, L.; Helson, H. E.; Hirthammer, M.; Mestdagh, H.; Spyroudis, S.; Vollhardt, K. P. C. *Angew. Chem., Int. Ed. Engl.* **1987**, *26*, 1246. (f) Schmidt-Radde, R. H.; Vollhardt, K. P. C. *J. Am. Chem. Soc.* **1992**, *114*, 9713. (g) Boese, R.; Matzger, A. J.; Mohler, D. L.; Vollhardt, K. P. C. *Angew. Chem., Int. Ed. Engl.* **1995**, *34*, 1478.

(11) Wilcox, C. F., Jr.; Grantham, G. D. *Tetrahedron* **1975**, *31*, 2889. Obendorf, S. K.; Wilcox, C. F., Jr.; Grantham, G. D.; Hughes, R. E. *Tetrahedron* **1976**, *32*, 1327. Wilcox, C. F., Jr.; Farley, E. N. *J. Am. Chem. Soc.* **1983**, *105*, 7191. Wilcox, C. F., Jr.; Lassila, K. R.; VanDuyne, G.; Lu, H.; Clardy, J. *J. Org. Chem.* **1989**, *54*, 2190.

**Table 1.** Selected Results of Calculations for Oligomers **6** and **8** and UV−vis Spectroscopic Data for 3,6-Di-*tert*-butylbiphenylene, Dimer **8** ($n = 2$), and Dimer **9** in THF[a]

| | Results of Calculations | | | | | | |
|---|---|---|---|---|---|---|---|
| | biphenylene | **8** ($n = 2$) | **8** ($n = 3$) | **8** ($n = 4$) | **8** ($n = 5$) | **6** ($n = 2$) | **6** ($n = 3$) |
| $\Delta H_f$ (grad) | 94.6 (0.8)[b] | 199.1 (2.0) | 303.4 (1.7) | 410.8 (36.8) | 519.5 (39.0) | 168.9 (1.2) | 243.7 (2.6) |
| HOMO−LUMO | 2.28 | 1.66 | 1.48 | 1.39 | 1.25 | 1.41 | 0.91 |

| | UV−Vis Data: $\lambda_{max}$ (nm) |
|---|---|
| 2,7-di-*tert*-butylbiphenylene | 364, 344, 330 |
| **8** ($n = 2$)[c] | 426, 405, 387 (sh) |
| **9**[c] | 429, 407, 386 |

[a] Heats of formation ($\Delta H_f$, kcal/mol) and gradient norms (grad) at the MNDO level of theory. HOMO−LUMO gaps (eV) at the EHT/MNDO level. [b] Experimental $\Delta H_f$; see ref 15. [c] Weak 495-nm (2.51 eV) and 462-nm maxima in the absorption curve are also observed in samples of **9**; single HPLC peaks (both normal and reversed phases) are found in these samples. Analogous bands are observed for **8** ($n = 2$).

Polymer **5** might be expected to possess localized $\pi$-bonding, analogous to **4**. An interesting question arises whether such localization within each biphenylene moiety might lead to a large density of states at the energies near the Fermi level, a feature of electronic structure associated with important materials properties.[13]

We now report the synthesis and study of biphenylene dimers **8** ($n = 2$) and **9**, which may be considered "macrocyclic" 2 × 2 fragments of net **1** and dimeric fragments of doubly-stranded polymer **5**. The electronic structure for polymer **5** is evaluated by band structure calculations at the extended Hückel theory (EHT) level.

## Results

**1. Calculations.** Planar geometries for biphenylene oligomers **8** ($n = 1-5$) and **6** ($n = 1-3$) are optimized at the MNDO level.[14] For selected oligomers, dimer **8** ($n = 2$) and trimer **6** ($n = 3$), vibrational frequencies are calculated; the $D_{2h}$-symmetric structures are minima on the potential energy surface, but some vibrational modes, corresponding to the out-of-plane distortions of the $\pi$-conjugated systems, are quite soft ($\nu < 40$ cm$^{-1}$); for comparison, the softest mode in biphenylene has $\nu \approx 117$ cm$^{-1}$ at this level of theory. The differences in propensity toward out-of-plane distortion for the biphenylene moiety for the molecules with varying numbers of biphenylene moieties are also found in the structures derived from single-crystal X-ray crystallography.[10c,g,12] It will be assumed that the planar structures ($D_{2h}$) satisfactorily represent all oligomers **8** and **6**. The heat of formation increments per $C_6H_2$ fragment are in the ranges 53 ± 1 and 75 ± 1 kcal/mol for oligomers **8** and **6** (Table 1),[15] respectively, reflecting different energies associated with $\pi$-conjugation and strain for these two types of oligomers.[6,7]

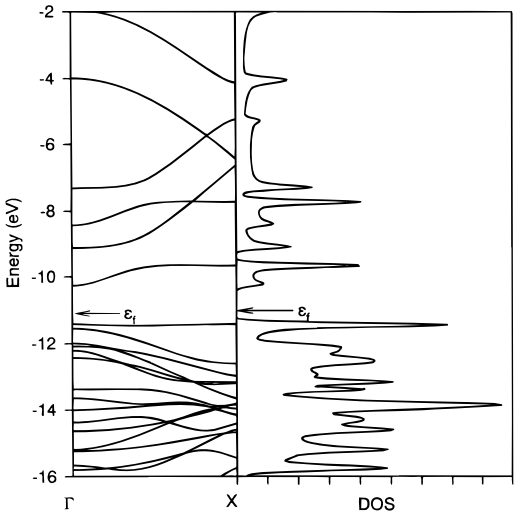


**Figure 1.** 1D polymer **5**: (left) band structure; (right) DOS profile at the EHT level of theory.

Calculations at the EHT level are carried out at the MNDO $D_{2h}$-symmetric geometries;[16] for polymer calculations, the geometries derived from the center repeat units of trimer **8** ($n = 3$) and dimer **6** ($n = 2$) are used. The decreases of the HOMO−LUMO gap, as a function of oligomer size, are less for oligomers **8** compared to those for oligomers **6** (Table 1). Band structure calculations (EHT) give the band gaps, $\Delta E_g =$ 1.1 and 0.0 eV, for the polymers **5** and **3**.[17]

With the increasing size of oligomers **8**, the near degeneracy of the HOMO becomes greater; e.g., for $n = 2-5$, the number of $\pi$-MOs within <0.07 eV of the HOMO energy is 1−4. This "clustering" of $\pi$-MOs near the HOMO in the oligomers is reflected in the band structure in polymer **5**; that is, a localized band near the Fermi level, leading to a large density of states (DOS) near the Fermi level, is found (Figure 1). Such electronic structure of a polymer is very promising for important materials properties.

**2. Synthesis.** The convergent synthesis of dimers **8** ($n = 2$) and **9** is based on three symmetrical aryl−aryl coupling steps (Figure 2). After Li/I or Li/Br exchange, the resultant aryllithiums are oxidized with Cu(II) (first and third steps) or converted to a cuprate with CuCN and, then, treated with oxygen

(12) The biphenylene framework may undergo "out-of-plane" distortion but with difficulty: Vögtle, F.; Saimacher, K.; Peyerimhoff, S.; Hippe, D.; Puff, H.; Bullesbach, P. *Angew. Chem., Int. Ed. Engl.* **1987**, *26*, 470. Vögtle, F.; Schulz, J. E.; Rissanen, K. *J. Chem. Soc., Chem. Commun.* **1992**, 120. Saitmacher, K.; Schulz, J. E.; Nieger, M.; Vögtle, F. *J. Chem. Soc., Chem. Commun.* **1992**, 175.

(13) (a) The DOS at the Fermi level may be correlated with $T_C$ for superconductors, according to the BCS theory; e.g., see: Burdett, J. K. *Chemical Bonding in Solids*; Oxford: New York, 1995; p 181 and references therein. (b) A large DOS at the Fermi level, such as associated with narrow and partially-filled bands, is also relevant to magnetism; for a review on organic high-spin polyradicals, exhibiting near-degeneracies at the HOMO level, see: Rajca, A. *Chem. Rev.* **1994**, *94*, 871. Band structure calculations at the EHT level for model polymeric polyradicals: Yoshizawa, K.; Hoffmann, R. *Chem. Eur.* **1995**, *1*, 403.

(14) Dewar, M. J. S.; Thiel, W. *J. Am. Chem. Soc.* **1977**, *99*, 4899. Stewart, J. J. P. MOPAC 93.00 Manual, Fujitsu Limited, Tokyo, 1993.

(15) The experimental value of $\Delta H_f°$ for biphenylene is 99.88 kcal/mol; see: Pedley, J. B.; Naylor, R. D.; Kirby, S. P. *Thermochemical Data of Organic Compounds*; Chapman and Hall: London, 1986. Good, W. D. *J. Chem. Thermodyn.* **1978**, *10*, 275. The calculated value of $\Delta H_f°$ for biphenylene at the 6-31G*(RMP2-FC)//6-31G* level of theory is 99.8 kcal/mol; see: Schulman, J. M.; Disch, R. L. *J. Mol. Struct.*: *THEOCHEM* **1992**, *259*, 173.

(16) EHT programs: Wangbo, M. H.; Evain, M.; Hughbanks, T.; Kertesz, M.; Wijeyesekera, S.; Wilker, C.; Zheng, C.; Hoffmann, R. QCPE 571.

(17) For calculations of the band gap in polymers **3** and **4**, see: (a) Baumgarten, M.; Dietz, F.; Müllen, K.; Karabunarliev, S.; Tyutyulkov, N. *Chem. Phys. Lett.* **1994**, *221*, 71. (b) Trinajstic, N.; Schmalz, T. P.; Zivkovic, T. P.; Nikolic, S.; Hite, G. E.; Klein, D. J.; Seitz, W. A. *New J. Chem.* **1991**, *15*, 27.

**Table 2.** Selected CC Bond Lengths (Å) and Dihedral Angles (deg) for Two Polymorphs of **9**: **9A**, Space Group $P2_1/n$, and **9B**, Space Group $P2_1/c$)[a]

| | 9A | 9B | | 9A | 9B |
|---|---|---|---|---|---|
| C(1)−C(2) | 1.416(5) | 1.429(4) | C(2)−C(3) | 1.362(5) | 1.365(4) |
| C(3)−C(4) | 1.412(5) | 1.415(4) | C(4)−C(5) | 1.345(5) | 1.359(4) |
| C(5)−C(6) | 1.412(5) | 1.417(4) | C(6)−C(1) | 1.375(5) | 1.389(4) |
| C(3)−C(13a) | 1.510(5) | 1.513(4) | C(4)−C(14a) | 1.501(5) | 1.529(4) |
| | | | C(5)−C(4)−C(14a)−C(15a) | 7.0 | 11.7 |
| | | | C(2)−C(3)−C(13a)−C(12a) | 5.3 | 6.6 |

[a] Atom numbering is shown in Figure 3.

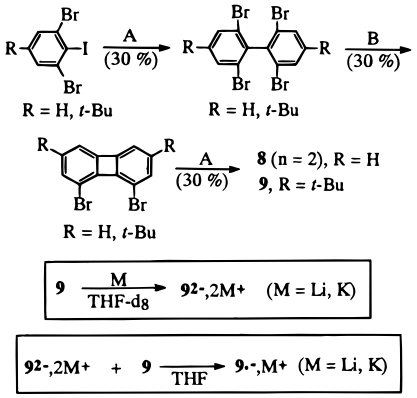


**Figure 2.** (Top) synthesis of biphenylene dimers **8** ($n = 2$) and **9**: (step A) (1) *n*-BuLi, ether, −78 °C, 2 h, (2) $CuBr_2$, from −78 °C to rt; (step B) (1) *n*-BuLi, THF, −78 °C, 2 h, (2) CuCN, from −78 °C to rt, (3) $O_2$, −78 °C. (Bottom, boxed equations) generation of dianion and radical anion of **9**.

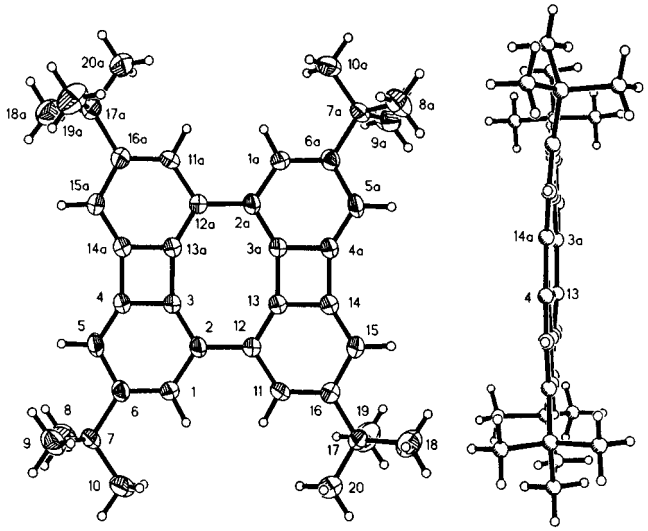

**Figure 3.** Molecular structure and conformation for biphenylene dimer **9**, obtained from the crystal structure of polymorph **9A** (space group $P2_1/n$): (left) frontal view; (right) side view. Carbon atoms in the frontal view are depicted with ellipsoids representing the 50% probability level. The molecule belongs to point group $C_i$; however, its $\pi$-conjugated part is approximately compatible with point group $C_{2h}$.

gas (second step).[18,19] NMR and MS data for products **8** ($n = 2$) and **9** support the proposed structures; X-ray crystallography for **9** confirms the structure (Figure 3, Table 2).

Three crystalline forms (polymorphs) of **9** are identified by measurements of lattice parameters: **9A**, **9B**, and **9C**. Polymorph **9A** is obtained by crystallization from solution; both **9B** and **9C** are obtained by heating **9A** to 380 °C under argon in a sealed tube. For polymorphs **9A** and **9B**, X-ray single-crystal structures are obtained. In both **9A** and **9B**, the $\pi$-conjugated moieties are distorted from planarity; that is, the two biphenylene moieties of each molecule are curved with the opposite sign curvatures. Two dihedral angles for the biphenyl moiety ("outer" side, C1−C2−C12−C11, and "inner" side, C3−C2−C12−C13), which should be exactly zero for the planar structure, may be used as an approximate measure of curvature (Figure 3). In **9A** (angles 7.0° and 5.3°), there is less curvature than in **9B** (angles 11.7° and 6.6°) (Table 2). The C−C bond alternations in **9A**, **9B**, and biphenylene are similar (Table 2).[20]

In the UV−vis spectrum, a bathochromic shift is observed for **9** compared to 2,7-di-*tert*-butylbiphenylene in THF (Figure 4); an analogous spectrum is observed for **8** ($n = 2$).[21,22]

Cyclic voltammetry of **9** in THF/TBAP gives two reversible waves, which correspond to the radical anion and dianion; the large potential separation of 0.4 V suggests that preparation of the radical anion (under comparable conditions) will not be hampered by disproportionation to the dianion and the neutral molecule.[23,24] The reduction waves for **9** ($E_p = -1.75$ and $-2.16$ V) are shifted toward less negative potential compared to the reduction wave for 2,7-di-*tert*-butylbiphenylene ($E_p = -2.43$ V) (Figure 5).[25]

Treatment of **9** with Li or K metal in tetrahydrofuran-$d_8$ (THF-$d_8$) leads initially to a purple solution with a very broad $^1$H NMR spectrum.[26] Upon further exposure to the alkali metal, the color of the solution changes to brown and relatively sharp $^1$H and $^{13}$C NMR ({$^1$H} and DEPT) spectra are observed (Figure 6); the NMR spectral patterns are similar to those for **9**, except for the differences in chemical shifts,[27] and **9** is quantitatively recovered upon quenching with $I_2$.

These observations are consistent with the conversion of **9** to its dianion $\mathbf{9^{2-},2M^+}$ (M = Li, K) via an intermediate radical anion, $\mathbf{9^{\bullet -},M^+}$ (M = Li, K).

(18) Wittig, G.; Klar, G. *Liebigs Ann. Chem.* **1967**, *704*, 91.

(19) Lipshutz, B. H.; Siegmann, K.; Garcia, E.; Kayser, F. *J. Am. Chem. Soc.* **1993**, *115*, 9276.

(20) X-ray structure for biphenylene: Fawcett, J. K.; Trotter, J. *Acta Crystallogr.* **1966**, *20*, 87.

(21) (a) The UV−vis spectrum for biphenylene in EtOH has been reported; at long $\lambda$, two band systems have been identified, a strong system with a band at 27 910 cm$^{-1}$ ($\lambda_{max} = 358$ nm, log $\epsilon \approx 4$, 3.46 eV) and a progression of weak bands starting at 25530 cm$^{-1}$ ($\lambda_{max} = 392$ nm, log $\epsilon \approx 2$, 3.16 eV): Carr, E. P; Pickett, L. W.; Voris, D. *J. Am. Chem. Soc.* **1941**, *63*, 3231. (b) The best value for energy of the 0,0 transition between the ground state, $S_{0,0}(A_g)$, and the lowest singlet excited state, $S_{1,0}(B_{1g})$, in biphenylene is estimated at 23 884 cm$^{-1}$ (2.96 eV) from the fluorescence spectra in 3-methylpentane at 130 K: Nickel, B.; Hertzberg, J. *Chem. Phys.* **1989**, *132*, 219.

(22) For the UV−vis spectra of $\pi$-conjugated hydrocarbons, their radical ions and diions, see: Perkampus, H.-H. *UV-VIS Atlas of Organic Compounds*; VCH: Weinheim, 1992.

(23) Rajca, S.; Rajca, A. *J. Am. Chem. Soc.* **1995**, *117*, 9172.

(24) Bard, A. J.; Faulkner, L. R. *Electrochemical Methods*; Wiley: New York, 1980.

(25) Analogously, the first and second reduction potentials for perylene (dimer of naphthalene) are less negative than the first reduction potential for naphthalene; for a compilation of electrochemical data on polycyclic aromatic hydrocarbons, see: Perichon, J. In *Polycyclic Aromatic Hydrocarbons* in *Encyclopedia of Electrochemistry of the Elements, Organic Section, Hydrocarbons and Hydroxy Compounds*; Bard, A. J., Lund, H., Eds.; Marcel Dekker, 1978; Vol. 11.

(26) LaMar, G. N.; Horrocks, D.; Holm, R. *NMR of Paramagnetic Molecules*; Academic Press: New York, 1973.

(27) Spiesecke, H.; Schneider, W. G. *Tetrahedron Lett.* **1961**, 468.

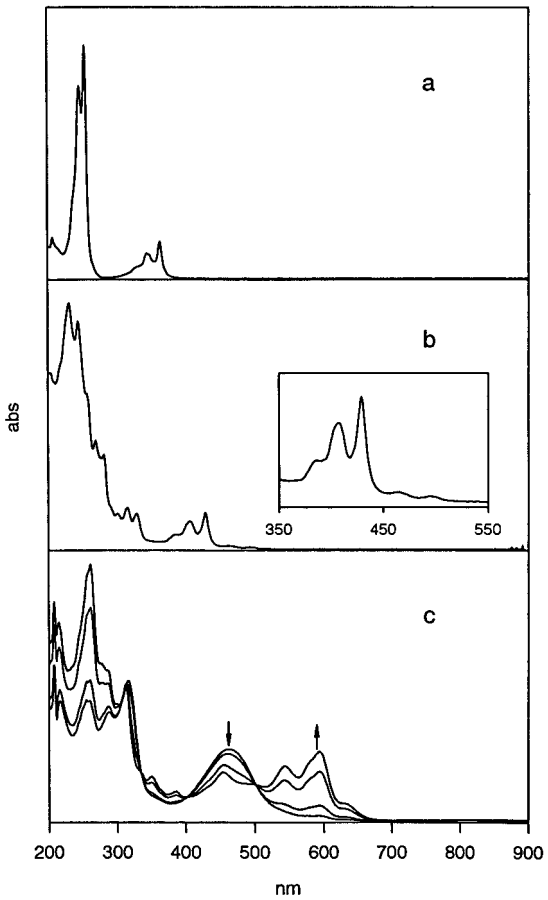


**Figure 4.** UV−vis spectroscopy: (a) 2,7-di-*tert*-butylbiphenylene in THF, (b) biphenylene dimer **9** in THF, (c) the reaction of disproportionation between dianion $\mathbf{9}^{2-}$,$\mathbf{2Li}^{+}$ in THF-$d_8$/THF and neutral **9** (via addition of solid **9** in small portions). Spectra a and b are summarized in Table 1. In spectra c, the initial and the final spectra correspond to $\mathbf{9}^{2-}$,$\mathbf{2Li}^{+}$ and $\mathbf{9}^{\bullet-}$,$\mathbf{Li}^{+}$, respectively.

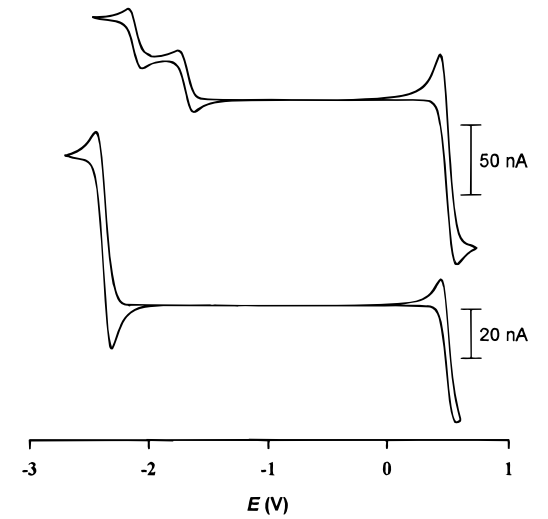


**Figure 5.** Cyclic voltammetry for **9** (top trace) and 2,7-di-*tert*-butylbiphenylene (bottom trace) in THF/TBAP with ferrocene as the reference (0.510 V vs SCE). Scan rates are 50 mV/s.

$\mathbf{9}^{\bullet-}$,$\mathbf{M}^{+}$ (M = Li, K) is most conveniently formed by adding solid **9** to a solution of $\mathbf{9}^{2-}$,$\mathbf{2M}^{+}$ (M = Li, K) in THF-$d_8$/THF. For the lithium salts (M = Li), the UV−vis spectra show that the absorbance of the $\lambda_{max}$ = 462 nm band of dianion $\mathbf{9}^{2-}$,$\mathbf{2Li}^{+}$ decreases and the $\lambda_{max}$ = 594 and 543 nm bands of radical anion $\mathbf{9}^{\bullet-}$,$\mathbf{Li}^{+}$ increase; the two longest $\lambda$ isosbestic points are observed at $\lambda$ = 502 and 403 nm (Figure 4).[28] The X-band ESR spectrum

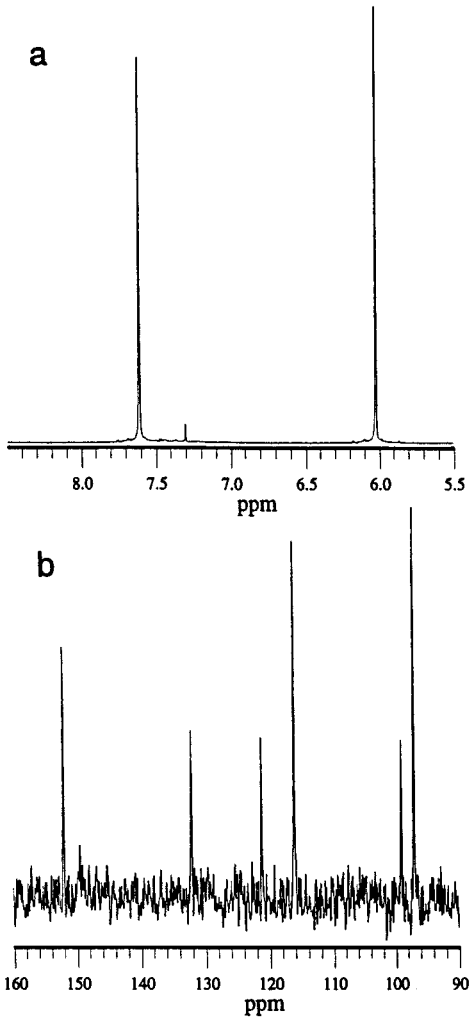


**Figure 6.** NMR spectra for dianion $\mathbf{9}^{2-}$,$\mathbf{2Li}^{+}$ in THF-$d_8$. (a) partial $^1$H NMR (500 MHz) spectrum; a small sharp peak at ~7.3 ppm is from a small amount of benzene in the sample; (b) partial $^{13}$C NMR (125 MHz) spectrum.

of the bright purple solution (corresponding to the final UV−vis spectrum in Figure 4) shows five lines ($a$ = 1.3 G) (Figure 7). Similar results are obtained for the potassium salts (M = K).

## Discussion

The band gap of polymer **5** may be estimated by comparing the calculational and experimental data. For both biphenylene and dimer **8** ($n$ = 2) the HOMO−LUMO excitation at the EHT/MNDO level of theory is electric dipole-forbidden ($B_{1g}$ excited state).[29] This is in qualitative agreement with the experiment for biphenylene, for which the longest $\lambda$ band in the UV−vis absorption spectrum at $\lambda_{max}$ = 392 nm (3.16 eV) is very weak.[21a] This weak band is not even discernible in the spectrum of 2,7-di-*tert*-butylbiphenylene in Figure 3. Thus, for biphenylene dimer **9**, the weak bands with $\lambda_{max}$ = 495 nm (2.51 eV) may correspond to the analogous electric dipole-forbidden transition.[30] Consequently, for biphenylene and its dimer, the calculated HOMO−LUMO gaps are underestimated vs the corresponding $\lambda_{max}$ by ca. 0.9 eV; this underestimate is 0.7 eV

(28) For a review on UV−vis spectroscopy of $\pi$-conjugated radical ions, see: Rao, C. N. R.; Kalyanaraman, V.; George, M. V. *Appl. Spectrosc. Rev.* **1970**, *3*, 153. See also ref 22.

(29) (a) The $x$ and $y$ axes are in the plane of the molecule, and the $x$ axis is taken as a long axis for the biphenylene moiety. (b) For calculations of UV−vis spectra for numerous biphenylene derivatives at the PPP level, see: Vogler, H.; Ege, G. *J. Am. Chem. Soc.* **1977**, *99*, 4599.

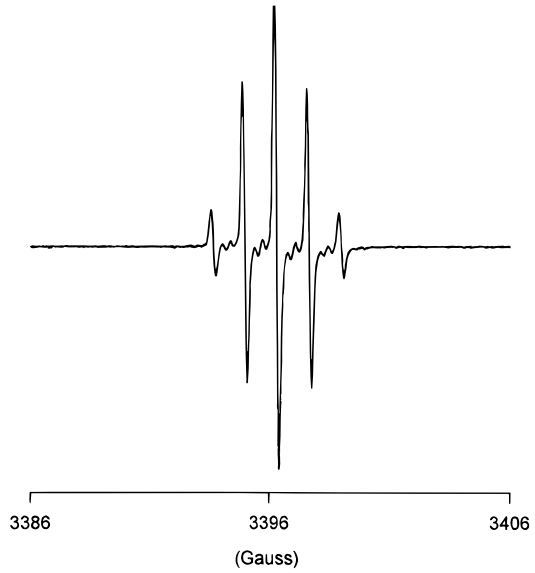


**Figure 7.** X-band ESR spectrum for radical anion $\mathbf{9}^{\bullet-}$,$\mathbf{Li}^{+}$ in THF-$d_8$/THF.

when the energy of the 0,0 transition in biphenylene is used for the comparison with the HOMO−LUMO gap.[21b] In conjunction with the calculated $\Delta E_g = 1.1$ eV, the current best estimate is $\Delta E_g \approx 2$ eV for polymer **5**; furthermore, the EHT band structure should qualitatively reflect the electronic structure of polymer **5**.[31,32]

The structure of **9** obtained from X-ray crystallography is a dimer of biphenylenes; the bond alternation, which may be viewed as a signature of localization, is similar in **9** and biphenylene. This structural interpretation is somewhat complicated by the nonplanarity of the biphenylene moieties in **9**. Dimer **9** may be considered as tetra-*o*-phenylene **10**,[33] "planarized" by biphenylene moieties; i.e., the dihedral angles between the benzene rings in tetra-*o*-phenylene are 65° vs <12° for **9**.[34] "Planarization" with five- or six-membered rings is expected to be less effective than that with the four-membered rings in **9**; the dihedral angles in **11** and **12** are intermediate

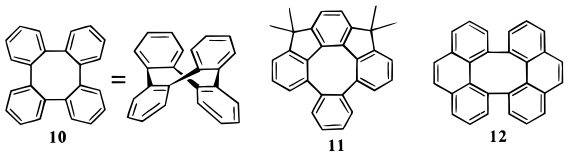


between those for **9** and **10**, according to X-ray crystallography.[35] Interestingly, out-of-plane distortions are helical in both **11** and **12**, but they are achiral in both polymorphs **9A** and **9B**.[35] MNDO calculations indicate a planar, but prone to out-of-plane distortion, structure for dimer **8** ($n = 2$). The softest vibrational mode ($A_u$, $\nu = 35$ cm$^{-1}$) is a helical out-of-plane distortion; the vibrational mode, corresponding to the achiral out-of-plane distortions in **9A** and **9B**, is significantly higher in energy ($B_{3g}$, $\nu = 96$ cm$^{-1}$) but still below the analogous mode in biphenylene ($B_{1u}$, $\nu = 117$ cm$^{-1}$). Are the out-of-plane distortions in polymorphs **9A** and **9B** caused by the crystal packing?

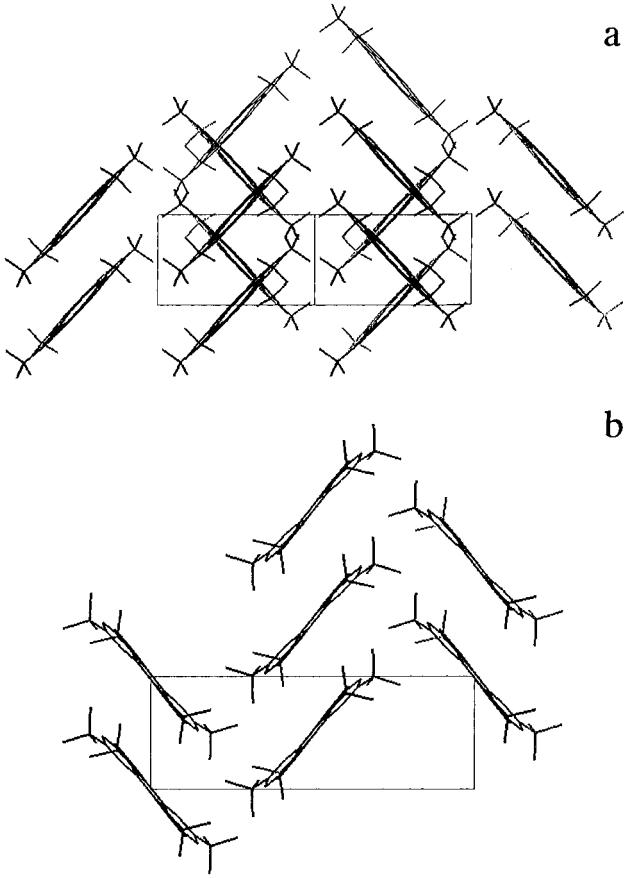


**Figure 8.** Crystal packing for polymorphs **9A** (a) and **9B** (b).

Crystal packings for polymorphs **9A** and **9B** consist of columnar stacks, which define the short axes (*b*) of the unit cells. Contacts between the stacks are similar to the herringbone pattern, forming the "quasi-two-dimensional" sheets of molecules; in **9A**, molecules show an alternating tilt within the sheet, and in **9B**, the tilt is uniform throughout the sheet (Figure 8). Although the *b* axes are longer than the upper limit of 5.4 Å for the $\gamma$ structures of typical aromatic hydrocarbons,[36] the intrastack interactions are important because of the bulkiness of the *tert*-butyl groups. Among the plethora of interstack and intrastack contacts, the cumulative effect of which is difficult to elucidate, the following intrastack interactions are identified as the most significant: (1) the *b* axis of ~6.0 Å in **9A** may be related to the presence of only one repulsive contact between the *tert*-butyl group and biphenylene moiety; (2) the *b* axis of ~6.2 Å in **9B** is accompanied by the presence of two dominant repulsive contacts between the *tert*-butyl groups of the neighboring molecules. These close contacts can approximately be described as follows:[37] in **9A**, the distances between one of the

(30) In biphenylene, the forbidden first electronic transition ($A_g-B_{1g}$) acquires some intensity via vibronic coupling with the allowed second electronic transition ($A_g-B_{3u}$): Yamaguchi, H.; Ata, M.; McOmie, J. F. W.; Barton, J. W.; Bauman, H. *J. Chem. Soc., Faraday Trans. 2* **1983**, *79*, 599.

(31) For the higher oligomers **8** ($n > 2$), the near degeneracy of the HOMO at the EHT/MNDO level does necessitate a higher level of theory, as typically needed for most $\pi$-conjugated systems, to predict the electronic spectra.

(32) For the oligomers related to polymer **3**, the discrepancies between the calculated and experimental energy gaps increase as a function of oligomer size; i.e., the electronic structure for polymer **3** is most likely not adequately described at the EHT level. It has been reported that, for polymer **3**, $\Delta E_g = 0.0$ eV at the simple $\pi$-Hückel level becomes ~2 eV when electron correlation is approximately accounted for (ref 17a).

(33) For a review on tetra-*o*-phenylenes, see: Mak, T. C. W.; Wong, H. N. C. *Top. Curr. Chem.* **1987**, *140*, 141.

(34) Irngartinger, H.; Reibel, W. R. K. *Acta Crystallogr. B* **1981**, *B37*, 1724.

(35) Irngartinger, H.; Reibel, W. R. K.; Sheldrick, G. M. *Acta Crystallogr. B* **1981**, *B37*, 1768. Wang, X.-M.; Hou, X.-L.; Zhou, Z.-Y.; Mak, T. C. W.; Wong, H. N. C. *J. Org. Chem.* **1993**, *58*, 7498.

(36) Desiraju, G. R.; Gavezotti, A. *Acta Crystallogr. B* **1989**, *B45*, 473.

(37) For the analysis of the crystal packing, standard CH bond distances of 1.09 Å were assummed.

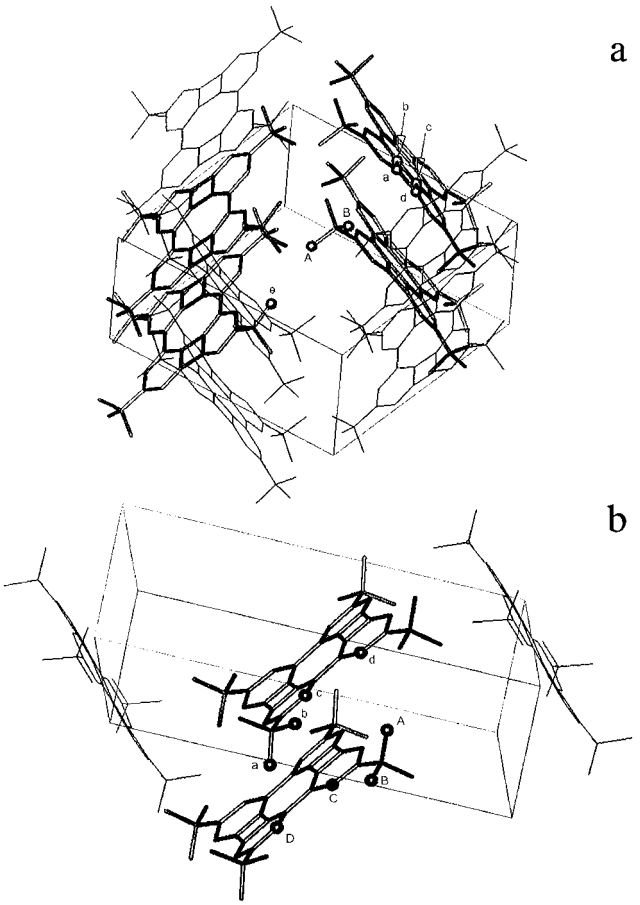


**Figure 9.** Close intermolecular contacts and out-of-plane distortions in polymorphs **9A** and **9B**: (a) **9A**, B−a (H−C, 2.67 Å), B−d (H−C, 2.71 Å), A−e (H−H, 2.62 Å); (b) **9B**, a−B (H−H, 2.44 Å), B−b (H−H, 2.58 Å), A−c (H−H, 2.58 Å), A−d (H−H, 2.54 Å), a−C (H−H, 2.60 Å), a−D (H−H, 2.68 Å).

hydrogen atoms of the *tert*-butyl group labeled B and carbon atoms labeled a and d are only ∼2.7 Å (Figure 9a), which is significantly less than the intermolecular C−H distance of ∼3.1 Å in the herringbone structure of benzene;[38] in **9B**, the distances between the nearest hydrogens of the *tert*-butyl groups labeled a and B (and the other symmetry-related pair of *tert*-butyl groups) are only ∼2.4 Å (Figure 9b).

The role of the *tert*-butyl groups in the crystal packing of **9A** and **9B** may be reflected in their torsional angles. Those *tert*-butyl groups, which are identified in the close contacts, have nonzero torques (23.3° in **9A**, 10.0° and 8.8° in **9B**), such as to somewhat alleviate the relevant repulsive interactions; e.g., for zero torsional angles, the close contacts B−a (∼2.7 Å), B-d (∼2.7 Å), and a−B (∼2.4 Å) would decrease to ∼2.3, ∼2.6, and ∼2.3 Å, respectively. (The two *tert*-butyl groups in **9A**, without readily recognizable close contacts, have torsional angles of 1.6°.)

Therefore, the repulsive intrastack contacts involving *tert*-butyl groups correlate with both the direction and the relative magnitudes of the out-of-plane distortions in **9A** and **9B** (Figure 9). An interesting predictive test of the above explanations would be the structure of dimer **8** ($n = 2$), some polymorphs of which should either be planar or possess small helical distortions.[39,40]

(38) Bacon, C. E.; Curry, N. A.; Wilson, S. A. *Proc. R. Soc. London, A* **1964**, *279*, 98.

(39) Herndon, W. C.; Nowak, P. C.; Connor, D. A.; Lin, P. *J. Am. Chem. Soc.* **1990**, *114*, 41. Goddard, R.; Haenel, M. W.; Herndon, W. C.; Kruger, C.; Zander, M. *J. Am. Chem. Soc.* **1995**, *117*, 30.

Dianions $\mathbf{9}^{2-}\mathbf{,2M}^{+}$ (M = Li, K) in THF-$d_8$ are persistent for at least several days at ambient temperature, unlike the previously reported dianions of biphenylene and its alkyl-substituted derivatives.[41] This observation is in accordance with the electrochemical data, i.e., a less negative potential for the formation of the dianion of **9** vs the monoanion of 2,7-di-*tert*-butylbiphenylene (Figure 5). Also, dianions $\mathbf{9}^{2-}\mathbf{,2M}^{+}$ (M = Li, K) have their counterpart among "planarized tetra-*o*-phenylenes", bis(fluorene) dianion **13**.[42]

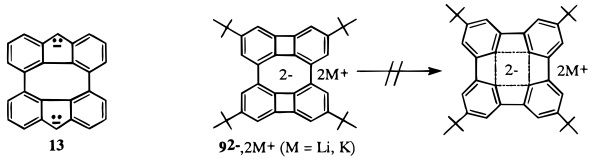


**13** $\mathbf{9}^{2-}\mathbf{,2M}^{+}$ (M = Li, K)

NMR spectra for dianions $\mathbf{9}^{2-}\mathbf{,2M}^{+}$ (M = Li, K) in THF-$d_8$ show 2-fold symmetric structure, compatible with the $\sigma$-framework identical to that of the neutral compound **9** (Figure 6). In particular, 4-fold-symmetric structures with a four-center electron sextet ("in-plane aromatic") are not found at the experimental conditions employed in this work.[43]

The negative spin/charge distributions are similar in radical anions $\mathbf{9}^{\bullet-}\mathbf{,M}^{+}$ (M = Li, K) and dianions $\mathbf{9}^{2-}\mathbf{,2M}^{+}$ (M = Li, K): (1) the X-band ESR spectrum for $\mathbf{9}^{\bullet-}\mathbf{,M}^{+}$ (M = Li, K) is consistent with hyperfine coupling of four equivalent protons ($a$ = 1.3 G); (2) in the $^{13}$C NMR spectrum of $\mathbf{9}^{2-}\mathbf{,2M}^{+}$ (M = Li, K), only one nonquaternary (CH) $^{13}$C resonance in the aromatic region is strongly shifted upfield.[27] These experimental spin/charge distributions are qualitatively reproduced by the AO coefficients of the LUMO for **8** ($n = 2$) at both the EHT/MNDO and the MNDO levels, providing further support for the interpretation of the UV−vis spectrum of **9** and the estimate of the band gap for polymer **5**.

## Conclusions

Experimental studies on biphenylene dimer **9** and the related calculations at the EHT/MNDO level suggest that double-stranded polymer **5** and its oligomers **8** should be important synthetic targets for materials with interesting electronic properties. One of the key questions to answer is whether p-doped (to radical cation, etc.) polymer **5** would be a 1D metal with a large DOS at the Fermi level.[44] Higher homologues of **9** should be readily attainable by modification of the synthetic route to dimer **9**. Topological near degeneracies in such oligomers (corresponding to a large DOS in the polymer), upon p-doping and crystallization, may lead to materials with interesting properties.[4]

The general idea of relating chemical bonding in molecules and solids has plenty of precedence.[45] In the context of the present work, the most basic concepts of bonding in organic chemistry, such as resonance and aromaticity/antiaromaticity, may provide guidance for the design of extended structures with a large DOS at the Fermi level. However, the consequences of

(40) No suitable single crystals for X-ray crystallography were grown for **8** ($n = 2$).

(41) Biphenylene dianions: Günther, M.-E.; Aydin, R.; Buchmeier, W.; Engelen, B.; Günther, H. *Chem. Ber.* **1984**, *117*, 1069. Benken, R.; Finneiser, K.; Puttkamer, H.; Günther, H.; Eliasson, B.; Edlund, U. *Helv. Chim. Acta* **1986**, *69*, 955. Bausch, J. W.; Gregory, P. S.; Olah, G. A.; Prakash, G. K. S.; Schleyer, P. v. R.; Segal, G. A. *J. Am. Chem. Soc.* **1989**, *111*, 3633.

(42) Hellwinkel, D.; Haas, G. *Liebigs Ann. Chem.* **1979**, 145.

(43) For a review on "in-plane aromaticity", see: Minkin, V. I.; Glukhovtsev, M. N.; Simkin, B. Y. *Aromaticity and Antiaromaticity*; Wiley: New York, 1994; Chapter 8.

(44) Roth, S. *One-Dimensional Metals*; VCH: New York, 1995.

(45) Hoffman, R. *Solids and Surfaces*; VCH: New York, 1988.

a large DOS at the Fermi level in solids (superconductor, metal, ferromagnet, etc.) are difficult to predict. Although for a class of oligomers with topological multi near degeneracies, such as organic high-spin molecules, strong electron localization and ferromagnetic spin coupling are predictable from the molecular topology;[13b,23] i.e., in this case, straightforward models can sufficiently account for the effects of electron−electron repulsion.[46]

Dissections of net **1** into polymers **3** and **5**, and then into a molecular fragment, biphenylene dimer **8** ($n = 2$), can be compared to those of the graphite net, poly(*peri*-naphthalene), and, then, perylene (naphthalene dimer).[47] At the molecular level, the biphenylene dimer and naphthalene dimer have quite different electronic structures; the differences for the polymers and nets remain to be determined.[48]

## Experimental Section

**General Procedures.** Ether and tetrahydrofuran (THF) for use on a vacuum line were distilled from sodium/benzophenone in a nitrogen atmosphere. Major chemicals were obtained from Aldrich. 1-Iodo-2,6-dibromobenzene and 1-iodo-2,6-dibromo-4-*tert*-butylbenzene were prepared using standard procedures of functional group transformations; starting materials were sulfanilamide (or 2,6-dibromoaniline) and *tert*-butylbenzene, respectively.[49−51] The vacuum lines and glovebox are described elsewhere.[23]

NMR spectra were obtained using Omega spectrometers ($^1$H, 500 and 300 MHz) in either $CDCl_3$ or THF-$d_8$; the chemical shift references were as follows: ($^1$H) TMS, 0.0 ppm ($CDCl_3$); THF-$d_7$, 3.58 ppm (THF-$d_8$); ($^{13}$C) $CDCl_3$, 77.0 ppm; THF-$d_8$, 67.45 ppm.

ESR spectra were acquired with a Bruker 200D X-band instrument at ambient temperature, using 4-mm CFQ tubes equipped with high-vacuum PTFE stopcocks (Kontes).

UV−vis absorption spectra were recorded at ambient temperature in a 2-mm-path-length quartz cell using a Perkin-Elmer Lambda 6 spectrophotometer. The quartz cell was equipped with high-vacuum PTFE stopcocks (Kontes). The spectrophotometer sample chamber was accessible from a Vacuum Atmospheres glovebox.

Cyclic voltammograms were recorded using a PARC 270 electrochemistry system at a 100-mm-diameter. Pt-disk working electrode in THF/TBAP (TBAP = tetrabutylammonium perchlorate) at ambient temperature; ferrocene (0.510 V vs SCE) was used as a reference.

HPLC was carried out using a Waters 600 instrument equipped with 8 × 10 Radial Pak Cartridges (NovaPak silica and NovaPak C18 with 4-$\mu$m particle sizes). For analysis of dimer **9**, the eluents were hexane (5.5 min at 0.8 mL/min) and acetonitrile/THF/water (65/30/5; 8.2 min at 2.0 mL/min).

Elemental analyses were carried out by Dr. G. M. Dabkowski, Director-Microlytics, P.O. Box 199, S. Deerfield, MA 01373, and M-H-W Laboratories, P.O. Box 15149, Phoenix, AZ 85060.

**X-ray Crystallography.** X-ray diffraction data were collected with a Siemens P4 automatic diffractometer using graphite-monochromatized Mo K$\alpha$ radiation ($\lambda = 0.710\,73$ Å). The crystal of **9A** was an orange prism, 0.6 × 0.2 × 0.1 mm$^3$; its space group was determined to be $P2_1/n$ with $a = 15.420(2)$ Å, $b = 5.967(1)$ Å, $c = 16.735(2)$ Å, $\beta = 102.478(7)°$, $Z = 2$, and $\rho_{calc} = 1.159$ Mg m$^{-3}$. The crystal of **9B** was a yellow-orange plate, 0.38 × 0.15 × 0.1 mm$^3$; its space group was determined to be $P2_1/c$ with $a = 14.423(1)$ Å, $b = 6.1657(6)$ Å, $c = 17.994(1)$ Å, $\beta = 104.125(5)°$, $Z = 2$, and $\rho_{calc} = 1.123$ Mg m$^{-3}$. The crystal of **9C** was an orange plate, 0.3 × 0.3 × 0.06 mm$^3$; its space group was determined to be $P2_1/n$ with $a = 14.856(4)$ Å, $b = 12.727(5)$ Å, $c = 17.198(5)$ Å, $\beta = 103.379(7)°$, and presumably $Z = 4$. The crystals were selected from the following two samples: (1) **9A**, obtained by slow evaporation of organic solvents (methylene chloride and ether), (2) **9B** and **9C**, obtained by heating under Ar at 380 °C.

The initial structure models were determined by direct methods, developed by Fourier methods, and refined by full-matrix least-squares techniques. Hydrogen atom positions were calculated from known geometry ($d_{C-H} = 0.96$ Å); H atoms were refined using a riding-atom model and two isotropic $U$ parameters (one for the methyl hydrogens, the second for the aromatic hydrogens). The carbon atoms were refined with anisotropic atomic displacement parameters.

For **9A**, final cycles were weighted $\{w^{-1} = \sigma^2(F) + 0.0006F^2\}$. Refinement of 183 variables converged to $R = 0.0529$, $wR = 0.0563$, and $S = 1.21$. For **9B**, final cycles were weighted $\{w^{-1} = \sigma^2(F) + 0.0007F^2\}$. Refinement of 183 variables converged to $R = 0.0539$, $wR = 0.0611$, and $S = 1.24$. For **9C**, only the unit cell and space group are known at this time.

Data collection and analysis are described in detail in deposited material. Fractional atomic coordinates, atomic displacement parameters, and parameters describing the bonding geometry and conformation are available as supporting information.

**2,2′,6,6′-Tetrabromo-4,4′-di-*tert*-butylbiphenyl.** *n*-BuLi (5.74 mL of a 2.5 M solution in hexane, 14.4 mmol) was added to a solution of 1-iodo-2,6-dibromo-4-*tert*-butylbenzene (5.00 g, 12.0 mmol) in ether (180 mL) at −78 °C. After the solution was stirred for 2 h at −78 °C, $CuBr_2$ (16.2 g, 72.0 mmol) was added, and then the reaction mixture was allowed to attain ambient temperature over a 12-h period. Cold water was added to the reaction mixture, and usual aqueous workup gave 4.47 g of a yellow oil. Treatment of the crude product with cold hexane (30 mL) afforded 1.04 g (30%) of a white solid. Mp: 269−271 °C. Anal. Calcd for $C_{20}H_{22}Br_4$: C, 41.27; H, 3.81. Found: C, 41.31; H, 3.99. LR/HR EIMS: *m*/*z* (ion type, % RA for *m*/*z* = 50−600, deviation for the formula) 581.840 40 ($(M + 4)^+$, 45%, −2.2 ppm deviation for $^{12}C_{20}{}^1H_{22}{}^{79}Br_2{}^{81}Br_2$), 579.842 47 ($(M + 2)^+$, 31%, −1.9 deviation for $^{12}C_{20}{}^1H_{22}{}^{79}Br_3{}^{81}Br_1$), 577.844 07 ($M^+$, 8%, −2.5 ppm deviation for $^{12}C_{20}{}^1H_{22}{}^{79}Br_4$), 566.822 16 ($(M + 4 - CH_3)^+$, 100%, 7.0 ppm deviation for $^{12}C_{19}{}^1H_{19}{}^{79}Br_2{}^{81}Br_2$), 562.824 78 ($(M - CH_3)^+$, 17%, 4.9 ppm deviation for $^{12}C_{19}{}^1H_{19}{}^{79}Br_4$). $^1$H NMR ($CDCl_3$): $\delta$ 7.63 (s, 4 H), 1.35 (s, 18 H). $^{13}C\{^1H\}$ NMR ($CDCl_3$): $\delta$ 154.6, 139.2, 129.0, 124.1, 35.0, 31.1.

**2,2′,6,6′-Tetrabromobiphenyl.** The crude product was obtained using the procedure analogous to that for the *tert*-butyl-substituted derivative; either $CuBr_2$ or $CuCl_2$ was used as the oxidant. From six reactions, using $CuCl_2$ as the oxidant, a white precipitate (9.03 g, 33%) from hexane was obtained. Mp: 214−216 °C (lit.[52] mp: 215 °C). $^1$H NMR ($CDCl_3$): $\delta$ 7.66 (d, $J = 8$ Hz, 4 H), 7.16 (t, $J = 8$ Hz, 2 H). GC−MS (EI): 470.

Column chromatography (flash silica, hexane) of the mother liquid allows for isolation of additional amounts of 2,2′,6,6′-tetrabromobiphenyl (overall yield 40+%) and the major side products.

**2-Chloro-1,3-dibromobenzene ($CuCl_2$ as Oxidant).** $^1$H NMR (500 MHz, $CDCl_3$): $\delta$ 7.58 (d, $J = 8$ Hz, 2 H), 6.98 (t, $J = 8$ Hz, 1 H). GC−MS (EI): *m*/*z* 271.

**1,2,3-Tribromobenzene ($CuBr_2$ as Oxidant, 25%).** $^1$H NMR ($CDCl_3$): $\delta$ 7.58 (d, $J = 8$ Hz, 2 H), 7.03 (t, $J = 8$ Hz, 1 H). GC−MS (EI): *m*/*z* 314, 316.

**1,8-Dibromo-3,6-di-*tert*-butylbiphenylene.** *n*-BuLi (3.44 mL of a 2.5 M solution in hexane, 8.59 mmol) was added to a solution of 2,2′,6,6′-tetrabromo-4,4′-di-*tert*-butylbiphenyl (2.00 g, 3.44 mmol) in THF (200 mL) at −78 °C. After the mixture was stirred for 2 h at −78 °C, CuCN (0.77 g, 8.6 mmol) was added and the mixture was allowed to warm to room temperature. After the CuCN had completely dissolved (red color solution), the reaction was recooled to −78 °C

(46) Borden, W. T.; Davidson, E. R. *J. Am. Chem. Soc.* **1977**, *99*, 4587. Ovchinnikov, A. A. *Theor. Chim. Acta* **1978**, *47*, 297. Klein, D. J.; Nelin, C. J.; Alexander, S.; Matsen, F. A. *J. Chem. Phys.* **1982**, *77*, 3101. Borden, W. T.; Iwamura, H.; Berson, J. A. *Acc. Chem. Res.* **1994**, *27*, 109.

(47) Poly(*peri*-naphthalene) and oligomers: Viruela-Martin, R.; Viruela-Martin, P. M.; Orti, E. *J. Chem. Phys.* **1992**, *97*, 8470. Baumgarten, M.; Koch, K. -H.; Müllen, K. *J. Am. Chem. Soc.* **1994**, *116*, 7341.

(48) Both net **1** and graphite are metals ($E_g = 0$) at the EHT level; for calculations on graphite, see: Whangbo, M.-H.; Hoffmann, R.; Woodward, R. B. *Proc. R. Soc. London, A* **1978**, *366*, 23. However, the electronic structure of net **1**, composed of polymer **3**, may not be adequately described at this level of theory.

(49) Seikel, M. K. *Organic Syntheses;* Wiley: New York, 1955; Collect. Vol. III, p 262.

(50) Shoesmith, J. B.; Mackie, A. *J. Chem. Soc.* **1928**, 2334.

(51) Drake, N. L.; Eaker, C. M.; Garman, J. A.; Hamlin, K. E., Jr.; Hayes, R. A.; Haywood, S. T.; Peck, R. M.; Preston, R. K.; Sterling, J., Jr.; van Hook, J. O.; Walton, E. *J. Am. Chem. Soc.* **1946**, *68*, 1602.

(52) Meyer, R; Meyer, W. *Chem. Ber.* **1920,** *53*, 2034−2052.

and dry $O_2$ was bubbled through the reaction mixture for 1 h. Subsequently, the dark-colored reaction mixture was allowed to warm to ambient temperature. The usual aqueous workup was followed with flash chromatography (silica gel) using hexane. The product was obtained as a powder, 0.485 g (33%). Mp: 102−104 °C. Anal. Calcd for $C_{20}H_{22}Br_2$: C, 56.90; H, 5.25. Found: C, 56.85; H, 5.26. GC−MS (CI): *m*/*z* 422. $^1$H NMR ($CDCl_3$): $\delta$ 6.79 (d, $J$ = 1 Hz, 2 H), 6.70 (d, $J$ = 1 Hz, 2 H), 1.23 (s, 18 H). $^{13}C\{^1H\}$ NMR ($CDCl_3$): $\delta$ 154.3, 150.8, 145.9, 128.2, 114.7, 109.6, 35.3, 30.8.

**1,8-Dibromobiphenylene.** Preparation of the crude product and its purification were carried out according to the procedure for the *tert*-butyl-substituted product. From three reactions, 1.90 g (34%) of a yellow powder (mp 145−146 °C) was obtained. $^1$H NMR (500 MHz, $CDCl_3$): $\delta$ 6.84 (d, $J$ = 8.5 Hz, 2 H), 6.65 (dd, $J_1$ = 8.5 Hz, $J_2$ = 7 Hz, 2 H), 6.83 (d, $J$ = 7 Hz). $^{13}C\{^1H\}$ NMR/DEPT (135°) (125 MHz, $CDCl_3$): $\delta$ 151.4 (q), 149.2 (q), 132.8, 130.4, 116.2, 110.2 (q). GC−MS (EI): *m*/*z* 310.

**Biphenylene Dimer 9.** *t*-BuLi (2.66 mL of a 1.7 M solution in pentane, 4.52 mmol) was added to a solution of 1,8-dibromo-3,6-di-*tert*-butylbiphenylene (0.457 g, 1.083 mmol) in ether (60 mL) at −78 °C. After the mixture was stirred for 2 h at −78 °C, $CuBr_2$ (1.46 g, 6.50 mmol) was added. The reaction mixture was allowed to attain ambient temperature over a 12-h period, and then cold water was added. The organic layer was washed with $HCl_{aq}$, water, and $Na_2CO_{3,aq}$ and then dried over $MgSO_4$. Concentration in vacuo afforded 0.2 g of a yellow oil. Recrystallization from hexane gave 97.5 mg (34%) of a yellow powder. Mp: >350 °C dec on air. The purity of the product was verified with both normal and reversed phase HPLC. Anal. Calcd for $C_{40}H_{44}$: C, 91.55; H, 8.45. Found: C, 90.23; H, 8.57. HR EIMS: *m*/*z* (ion type, % RA for *m*/*z* = 50−600, deviation for the formula) 525.348 69 ($(M + 1)^+$, 43%, 2.0 ppm deviation for $^{12}C_{39}{}^{13}C_1{}^1H_{44}$), 524.343 49 ($M^+$, 100%, −1.6 ppm deviation for $^{12}C_{40}{}^1H_{44}$), 509.321 66 ($(M - CH_3)^+$, 21%, 1.6 ppm deviation for $^{12}C_{39}{}^1H_{41}$). $^1$H NMR (500 MHz, $CDCl_3$): $\delta$ 6.71 (d, $J$ = 1 Hz, 4 H), 6.44 (d, $J$ = 1 Hz, 4 H), 1.22 (s, 36 H). $^{13}C\{^1H\}$ NMR ($CDCl_3$): $\delta$ 152.5, 150.5, 146.8, 125.0, 118.1, 115.2, 35.1, 30.8.

**Biphenylene Dimer 8 (*n* = 2).** The crude product was obtained using the procedure analogous to that for the *tert*-butyl-substituted derivative. Treatment with chloroform gave 0.25 g (30%) of a yellow powder (mp 330−335 °C dec) from three reactions. A sample for elemental analysis was sublimed under vacuum. The solubility of the product in most organic solvents is very low. Anal. Calcd for $C_{24}H_{12}$: C, 95.97; H, 4.03; Found: C, 95.60; H, 4.36. HR EIMS: *m*/*z* (ion type, % RA for *m*/*z* = 50−303, deviation for the formula) 301.097 44 ($(M + 1)^+$, 27%, 0.6 ppm deviation for $^{12}C_{23}{}^{13}C_1{}^1H_{12}$), 300.094 59 ($M^+$, 100%, 2.3 ppm deviation for $^{12}C_{24}{}^1H_{12}$). $^1$H NMR (500 MHz, $CDCl_3$): $\delta$ 6.73 (d, $J$ = 8.5 Hz, 4 H), 6.57 (dd, $J_1$ = 8.5 Hz, $J_2$ = 7 Hz, 4 H), 6.32 (d, $J$ = 7 Hz, 4 H).

**Dianion $9^{2-}$,$2M^+$ (M = Li, K) and Radical Anion $9^{\bullet-}$,$M^+$ (M = Li, K): NMR, ESR, and UV−Vis Spectroscopies.** Freshly cut Li or K (multimolar excess) was added in a glovebox to a 5-mm NMR tube, containing solid **9** (∼5 mg) and equipped with a high-vacuum PTFE stopcock (Kontes). The piece of alkali metal was suspended in the upper part of the NMR tube. The tube was evacuated overnight, and then THF-$d_8$ (∼0.4 mL) was vacuum transferred from purple Na/benzophenone. The tube was flame sealed, and the NMR spectrum of **9** was recorded. $^1$H NMR (THF-$d_8$): $\delta$ 6.77 (s, 4 H), 6.49 (s, 4 H), 1.23 (s, 36 H). Subsequently, the piece of alkali metal was put in contact with the solution for 1−2 min until an intense purple color appeared. (For some samples, the alkali metal surface was activated by a brief sonication.) In the next step, the piece of alkali metal was suspended in the upper part of the NMR tube and an NMR spectrum was recorded. The reaction was continued until a relatively sharp NMR spectrum of $\mathbf{9^{2-},2M^+}$ (M = Li, K) was obtained.

**$9^{2-}$,$2Li^+$.** $^1$H NMR (THF-$d_8$): $\delta$ 7.61 (d, $J$ = 1 Hz, 4 H), 6.02 (d, $J$ = 1 Hz, 4 H), 1.41 (s, 36 H). $^{13}C\{^1H\}$ NMR/DEPT (135°): $\delta$ 152.0 (q), 132.1 (q), 121.2 (q), 116.2, 99.1 (q), 97.1, 35.8 (q), 32.3.

**$9^{2-}$,$2K^+$.** $^1$H NMR (THF-$d_8$): $\delta$ 7.74 (br s, 4 H), 6.17 (br s, 4 H), 1.42 (s, 36 H). $^{13}C\{^1H\}$ NMR/DEPT (135°): $\delta$ 151.0 (q), 133.5 (q), 119.0 (q), 116.2, 98.5 (q), 98.3, 35.8 (q), 32.1. (Further exposure of $\mathbf{9^{2-},2M^+}$ (M = Li, K) to alkali metal leads to the precipitation of unidentified product(s).) The NMR tube was promptly transferred to a glovebox, and its content was either quenched with $I_2$ or used for further UV−vis and ESR spectroscopic studies.

Upon dilution with THF, the UV−vis spectrum of $\mathbf{9^{2-},2M^+}$ (M = Li, K) was recorded. (The inner surfaces of quartzware and glassware were washed with a dilute solution of $\mathbf{9^{2-},2M^+}$ (M = Li, K), immediately prior to the experiments, in order to remove trace amounts of moisture and oxygen.) When solid **9** was added in small portions to the above dilute solution of $\mathbf{9^{2-},2M^+}$ (M = Li, K) in THF, the color of the solution gradually changed from yellow-brown to bright purple; the corresponding UV−vis spectra showed isosbestic points (e.g., spectra c in Figure 4). The bright purple solution gave a simple five-line ESR spectrum ($a$ = 1.3 G), as expected for radical anion $\mathbf{9^{\bullet-},M^+}$ (M = Li, K).

**Acknowledgment.** We gratefully acknowledge the National Science Foundation, Divisions of Materials Research and Chemistry, for support of this research (Grants DMR-9204826 and CHE-9510096 to A.R. and CHE- 9214428 to J.J.S.), including the GC−MS instrument (Instrumentation Program, Grant CHE-9300831). A.R. thanks the Center for Materials Research and Analysis at Nebraska for a "seed" grant. We acknowledge Pavel Bolshov, Ovanes Oganisian, and Philip Pazderka for their help with the synthesis. A.R. thanks Professor M. H. Whangbo (North Carolina State University) for examples of 2D and 3D input files for the EHT programs.

**Supporting Information Available:** Summary of the crystallographic data of **9A** and **9B** (17 pages). See any current masthead page for ordering and Internet access instructions.

JA961065Y